8

Carbon Nanotube Synthesis and Growth Mechanism

Mukul Kumar
Department of Materials Science & Engineering
Meijo University, Nagoya 468-8502
Japan

1. Introduction

A carbon nanotube (CNT) is a tubular structure made of carbon atoms, having diameter of nanometer order but length in micrometers. Right from its discovery, we have been listening exciting quotations about CNT, viz.

- "CNT is 100 times stronger than stainless steel and six times lighter..."
- "CNT is as hard as diamond and its thermal capacity is twice that of pure diamond..."
- "CNT's current-carrying capacity is 1000 times higher than that of copper..."
- "CNT is thermally stable up to 4000K..."
- "CNT can be metallic or semiconducting, depending on their diameter and chirality..."

However, it is important to note that all those superlative properties were predicted for an atomically-perfect *ideal* CNT which is far from the CNTs we are *practically* producing today. Despite a huge progress in CNT research over the years, we are still unable to produce CNTs of well-defined properties in large quantities by a cost-effective technique. The root of this problem is the lack of proper understanding of the CNT growth mechanism. There are several questions at the growth level awaiting concrete answer. Till date no CNT growth model could be robustly established. Hence this chapter is devoted to review the present state of CNT synthesis and growth mechanism.

There are three commonly-used methods of CNT synthesis. Arc-discharge method, in which the first CNT was discovered, employs evaporation of graphite electrodes in electric arcs that involve very high (~4000°C) temperatures (Iijima, 1991). Although arc-grown CNTs are well crystallized, they are highly impure; about 60–70% of the arc-grown product contains metal particles and amorphous carbon. Laser-vaporization technique employs evaporation of high-purity graphite target by high-power lasers in conjunction with high-temperature furnaces (Thess et al., 1996). Although laser-grown CNTs are of high purity, their production yield is very low (in milli gram order). Thus, it is obvious that these two methods score too low on account of efficient use of energy and resources. Chemical vapor deposition (CVD), incorporating catalyst-assisted thermal decomposition of hydrocarbons, is the most popular method of producing CNTs; and it is truly a low-cost and scalable technique for mass production of CNTs (Cassell et al., 1999). That is why CVD is the most popular method of producing CNTs nowadays. Here we will review the materials aspects of CNT synthesis by CVD and discuss the CNT growth mechanism in the light of latest progresses in the field.

2. CNT synthesis

Figure 1 shows a schematic diagram of the experimental set-up used for CNT growth by CVD method in its simplest form. The process involves passing a hydrocarbon vapor (typically 15–60 min) through a tubular reactor in which a catalyst material is present at sufficiently high temperature (600–1200°C) to decompose the hydrocarbon. CNTs grow on the catalyst in the reactor, which are collected upon cooling the system to room temperature. In the case of a liquid hydrocarbon (benzene, alcohol, etc.), the liquid is heated in a flask and an inert gas is purged through it, which in turn carries the hydrocarbon vapor into the reaction zone. If a solid hydrocarbon is to be used as the CNT precursor, it can be directly kept in the low-temperature zone of the reaction tube. Volatile materials (camphor, naphthalene, ferrocence etc.) directly turn from solid to vapor, and perform CVD while passing over the catalyst kept in the high-temperature zone. Like the CNT precursors, also the catalyst precursors in CVD may be used in any form: solid, liquid or gas, which may be suitably placed inside the reactor or fed from outside. Pyrolysis of the catalyst vapor at a suitable temperature liberates metal nanoparticles in-situ (such a process is known as floating catalyst method). Alternatively, catalyst-coated substrates can be placed in the hot zone of the furnace to catalyze the CNT growth.

CNT synthesis involves many parameters such as hydrocarbon, catalyst, temperature, pressure, gas-flow rate, deposition time, reactor geometry. However, to keep our discussion compact, here we will consider only the three key parameters: hydrocarbon, catalyst and catalyst support.

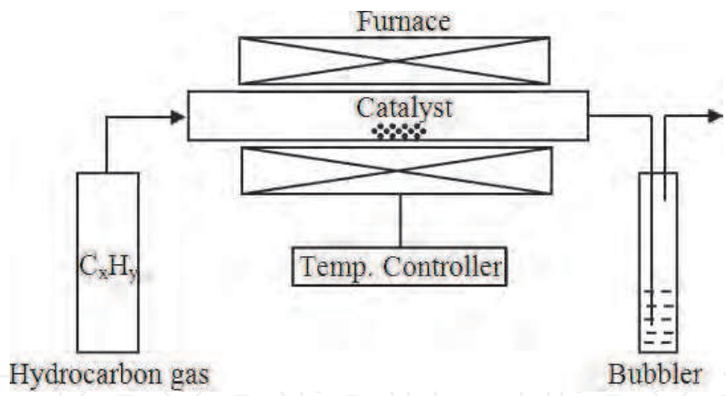

Fig. 1. Schematic diagram of a CVD setup in its simplest form.

2.1 CNT precursors

Most commonly used CNT precursors are methane, ethylene, acetylene, benzene, xylene and carbon monoxide. Among the early reports of CVD, MWCNTs were grown from the pyrolysis of benzene at 1100°C (Endo et al., 1991) and from acetylene at 700°C (Jose-Yacaman et al., 1993). In those cases, iron nanoparticles were used as the catalyst. Later, MWCNTs were also grown from many other precursors including cyclohexane (Li et al., 2007) and fullerene (Nerushev et al., 2003). On the other hand, SWCNTs were first produced from the disproportionation of carbon monoxide at 1200°C, in the presence of molybdenum nanoparticles (Dai et al., 1996). Later, SWCNTs were also produced from benzene, acetylene, ethylene, methane, cyclohexane, fullerene etc. by using various catalysts. In 2002, a low-temperature synthesis of high-purity SWCNTs was reported from alcohol CVD on Fe-Co-

impregnated zeolite support (Maruyama et al., 2002); and since then, ethanol became the most popular CNT precursor in the CVD method worldwide. Special feature of ethanol is that ethanol-grown CNTs are almost free from amorphous carbon, owing to the etching effect of OH radical. Later, vertically-aligned SWCNTs were also grown on Mo-Co-coated quartz and silicon substrates (Murakami et al., 2004). Recently, it has been shown that intermittent supply of acetylene in ethanol CVD significantly assists ethanol in preserving the catalyst's activity and thus enhances the CNT growth rate (Xiang et al., 2009).

The molecular structure of the precursor has a detrimental effect on the morphology of the CNTs grown (K. Ghosh et al., 2009). Linear hydrocarbons such as methane, ethylene, acetylene, thermally decompose into atomic carbons or linear dimers/trimers of carbon, and generally produce straight and hollow CNTs. On the other hand, cyclic hydrocarbons such as benzene, xylene, cyclohexane, fullerene, produce relatively curved/hunched CNTs with the tube walls often bridged inside.

General experience is that low-temperature CVD (600–900°C) yields MWCNTs, whereas high-temperature (900–1200°C) reaction favors SWCNT growth. This indicates that SWCNTs have a higher energy of formation (presumably owing to small diameters; high curvature bears high strain energy). Perhaps that is why MWCNTs are easier to grow (than SWCNTs) from most of the hydrocarbons, while SWCNTs grow from selected hydrocarbons (viz. carbon monoxide, methane, etc. which have a reasonable stability in the temperature range of 900–1200°C). Commonly efficient precursors of MWCNTs (viz. acetylene, benzene, etc.) are unstable at higher temperature and lead to the deposition of large amounts of carbonaceous compounds other than the nanotubes.

In 2004, a highly-efficient synthesis of impurity-free SWCNTs was reported by water-assisted ethylene CVD on Si substrates (Hata et al., 2004). It was proposed that controlled supply of steam into the CVD reactor acted as a weak oxidizer and selectively removed amorphous carbon without damaging the growing CNTs. Balancing the relative levels of ethylene and water was crucial to maximize the catalyst's lifetime. Recently, however, it has been shown that a reactive etchant such as water or hydroxyl radical is not required at all in cold-wall CVD reactors if the hydrocarbon activity is low (Zhong et al., 2009). These studies emphatically prove that the carbon precursor plays a crucial role in CNT growth. Therefore, by proper selection of CNT precursor and its vapor pressure, both the catalyst's lifetime and the CNT-growth rate can be significantly increased; and consequently, both the yield and the quality of CNTs can be improved.

2.2 CNT catalysts

For synthesizing CNTs, typically, nanometer-size metal particles are required to enable hydrocarbon decomposition at a lower temperature than the spontaneous decomposition temperature of the hydrocarbon. Most commonly-used metals are Fe, Co, Ni, because of two main reasons: (i) high solubility of carbon in these metals at high temperatures; and (ii) high carbon diffusion rate in these metals. Besides that, high melting point and low equilibrium-vapor pressure of these metals offer a wide temperature window of CVD for a wide range of carbon precursors. Recent considerations are that Fe, Co, and Ni have stronger adhesion with the growing CNTs (than other transition metals do) and hence they are more efficient in forming high-curvature (low diameter) CNTs such as SWCNTs (Ding et al., 2008).

Solid organometallocenes (ferrocene, cobaltocene, nickelocene) are also widely used as a CNT catalyst, because they liberate metal nanoparticles in-situ which catalyze the hydrocarbon decomposition more efficiently. It is a general experience that the catalyst-

particle size dictates the tube diameter. Hence, metal nanoparticles of controlled size, pre-synthesized by other reliable techniques, can be used to grow CNTs of controlled diameter. Thin films of catalyst coated on various substrates are also proven good in getting uniform CNT deposits (Fan et al., 1999). The key to get pure CNTs is achieving hydrocarbon decomposition on the catalyst surface alone and prohibiting the aerial pyrolysis. Recently, a high-yield CNT growth has been observed from acetylene decomposition on a stainless steel sheet at 730°C, without using any additional catalyst (Camilli et al., 2011). This study proves that the catalyst as a whole does not necessarily need to be a nanoparticle. Even a bulk metal can catalyze the CNT growth provided that the surface roughness is on nanometer scale. Moreover, alloys are proven to have a higher catalytic activity than pure metals. In 2008, *gigas growth* of CNT was reported from Fe-Co catalyst on zeolite support resulting in a weight gain of 1000% and volume gain of 10,000%, relative to the zeolite bed (Kumar et al., 2008). Hence, by combining different metals in different ratios and carefully controlling the catalyst calcination conditions, it is possible to evolve new crystallographic phases that could exhibit much higher catalytic activity toward CNT growth. Very recently, highly active crystallographic phases of Co-Mo and Ni-Mo have been achieved on MgO support, yielding ~3000 wt% CNT growth (Nunez et al., 2011).

Apart from the popular transition metals (Fe, Co, Ni), other metals of this group, such as Cu, Au, Ag, Pt, Pd were also found to catalyze CNT growth from various hydrocarbons (Moisala et al., 2003). On the role of CNT catalysts, it is worth mentioning that transition metals are proven to be efficient catalysts not only in CVD but also in arc-discharge and laser-vaporization methods. Therefore, it is likely that these apparently different methods might inherit a common growth mechanism of CNT, which is not yet clear. Hence this is an open field of research to correlate different CNT techniques in terms of the catalyst's role in entirely different temperature and pressure range.

2.3 CNT catalyst supports

The same catalyst works differently on different support materials. Commonly used substrates in CVD are quartz, silicon, silicon carbide, silica, alumina, alumino-silicate (zeolite), $CaCO_3$, magnesium oxide, etc. For an efficient CNT growth, the catalyst-substrate interaction should be investigated with utmost attention. Metal–substrate reaction (chemical bond formation) would cease the catalytic behavior of the metal. The substrate material, its surface morphology and textural properties greatly affect the yield and quality of the resulting CNTs. Zeolite substrates with catalyst in its nanopores have resulted significantly high yields of CNTs with a narrow diameter distribution (Kumar et al., 2005). Alumina materials are reportedly a better catalyst support than silica owing to stronger metal-support interaction in the former, which allows high metal dispersion and thus a high density of catalytic sites. Such interactions prevent metal species from aggregating and forming unwanted large clusters that lead to graphite particles or defective MWCNTs. Recent in-situ XPS analysis of CNT growth from different precursors on iron catalyst supported on alumina and silica substrates have confirmed these theoretical assumptions. Thin Alumina flakes (0.04–4 μm thick) loaded with iron nanoparticles have shown high yields of aligned CNTs of high aspect ratio (Mattevi et al., 2008). Latest considerations are that the oxide substrate, basically used as a physical support for the metal catalyst, might be playing some chemistry in the CNT growth (Noda et al., 2007). Accordingly, the chemical state and structure of the substrate are more important than that of the metal.

The crystallographic orientation of the exposed substrate surface governs the CNT growth direction. CNTs preferentially grow at 90° to Si (100) surface, but at 60° to Si (111) surface (Su et al., 2000). While α-plane sapphire leads to CNT growth normal to (001), no orientation is observed on c-plane or m-plane sapphire (Han et al., 2005). Similarly, single-crystal MgO (001) substrate shows preferential growth of CNTs along [110] direction (Maret et al., 2007). Very recently, an orthogonal CNT growth has been observed on micro-sized alumina particles (Fig. 2) by CVD of ferrocene-xylene mixture at 600°C (He et al., 2011). This observation proves that the grain boundary or crystalline steps of the support material play a crucial role in CNT growth and orientation.

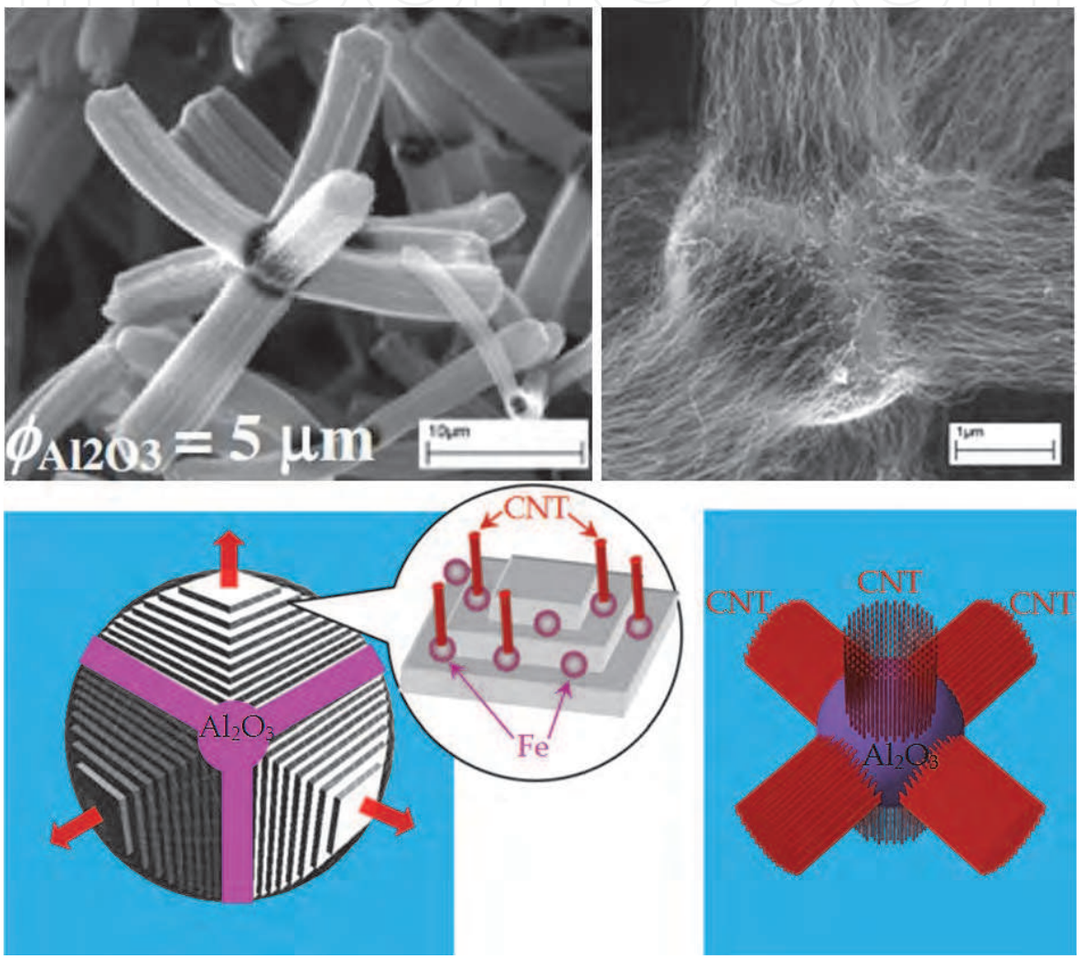

Fig. 2. Orthogonal growth of CNTs from an Al_2O_3 substrate. The crystalline steps of Al_2O_3 microparticle guide the direction of CNTs growing from the Fe nanoparticles lying on those steps. (He et al., 2011. Carbon 49, 2273-2286. © Elsevier Science).

2.4 New CNT catalysts

Recent developments in the nanomaterials synthesis and characterization have enabled many new catalysts for the CNT growth. Apart from popularly used transition metals (Fe, Co, Ni), a range of other metals (Cu, Pt, Pd, Mn, Mo, Cr, Sn, Au, Mg, Al) has also been successfully used for horizontally-aligned SWCNT growth on quartz substrates (Yuan et al.,

2008). Unlike transition metals, noble metals (Au, Ag, Pt, Pd etc.) have extremely low solubility for carbon, but they can dissolve carbon effectively for CNT growth when their particle size is very small (<5nm). Recently, a controlled growth of SWCNTs was reported on Au nanoparticles deposited on the atomic steps of Si (Takagi et al., 2008). It was found that the active catalyst is Au-Si alloy with about 80 at% Au.

Although copper is a transition metal, it showed insignificant catalytic effect on the CNT growth in the past (Vanderwal et al., 2001). In fact, it had been considered as an adverse contaminant. As a recent development, however, Cu has been found to catalyze the CNT growth efficiently. Methane and ethanol decomposition at 825–925°C on Cu nanoparticles supported on silicon wafers produced high densities of well-crystallined SWCNTs up to 1 cm in length (Zhou et al., 2006). The Cu nanoparticles were synthesized by the reduction of $CuCl_2$ in the presence of Cu_2O nanoparticles produced by thermolysis of cupric formates in coordinating solvents. This implies that the novelty lies in the catalyst-preparation method.

Rhenium (Re) is a rare catalyst used for CNT growth. Diamagnetic SWCNTs and MWCNTs were reported from methane decomposition on Re catalyst (Ritschel et al., 2007). The current scenario is that, just as any carbon-containing material can yield CNT, any metal can catalyze the CNT growth, provided that the experimental conditions are properly optimized. Accordingly, there is a huge scope in exploring new metals as CNT catalyst.

2.5 Metal-free CNT growth

Recently, nanodiamond particles (5 nm) were shown to catalyze the CNT growth (Takagi et al., 2009). Ethanol suspension of nanodiamond particles was spread on graphite plates and dried in air at 600°C. This resulted in isolated diamond particles, monolayers of diamond, and multilayered-diamond stacks on the substrate, depending upon the diamond concentration (0.01–1.0 wt%). Ethanol CVD over these diamond-loaded substrates at 850°C produced isolated CNTs, layered CNTs and high-density CNT mats, respectively. The nanodiamond particles do not fuse even after high-temperature CVD process, implying that they remain in solid state during CVD. Nanodiamond is therefore said to act as a CNT growth seed. This result proves that CNT growth is possible without metal catalyst. Does nanodiamond act as a catalyst? If it does, how? These are open questions.

In many studies, oxygen was noticed to activate the CNT growth. Recent studies have revealed that many metals, which do not exhibit catalytic activity in pure-metal form, do well in oxide form (Rummeli et al., 2005). Does metal oxide act as a catalyst? Template-free directional growth of CNTs has been achieved on sapphire (Han et al., 2005). CNTs have also been grown on semiconductors such as Si and Ge nanoparticles (though C has little solubility in bulk Si or Ge), provided that the nanoparticles are heated in air just before CVD (Takagi et al., 2007). Similarly, CNT growth on SiC substrates takes place only when some oxygen is present in the chamber (Kusunoki et al., 2000). Porous Al_2O_3 has already been shown to facilitate CNT growth without any catalyst (Schneider et al., 2008). Catalyst-free CNT growth is also possible in oxy-fuel flames (Merchan-Merchan et al., 2002). And oxide, typically used as a catalyst support in CVD, is itself capable of forming graphene layers (Rummeli et al., 2007a). All these examples resoundingly indicate that oxygen plays a key role in CNT growth. The question is whether oxygen is a catalyst! HRTEM investigation of the CNTs grown from cyclohexane pyrolysis over iron nanoparticles supported on thin Al_2O_3 layers shows that CNT keeps on growing even when the metal is completely

encapsulated in the tube center (Rummeli et al., 2007b). The authors propose that the metal only helps to initiate the CNT precipitation at the nucleation stage. Once the CNT head is created, metal becomes non functional; subsequent carbon addition to the CNT base periphery is facilitated from the substrate's oxide layer. This concept is radically different from the existing concept that the metal must remain exposed (either on the CNT tip or base) to keep the growth on. Hence more careful in-situ observation and robust theoretical support are required to establish the oxide's direct role as a catalyst.

More recent development of the field is even more exciting: CNT growth is possible with no metal at all; the non-metallic substrate itself acts as the CNT catalyst. Liu et al. (2009) passed methane and hydrogen (1:1) over an SiO_2-sputtered Si wafer at 900°C for 20 min and got dense SWCNTs grown on it. In the same CVD condition, thermally-grown SiO_2 films did not result CNTs. The success lies in the in-situ transformation of the sputtered SiO_2 film (30 nm) into isolated Si particles (1.9 nm) which efficiently catalyzed methane decomposition due to small-size effect. Similar SiO_2 nanoparticle generation and subsequent CNT growth was reported by another group from ethanol decomposition on annealed SiO_2/Si substrates (Liu et al., 2010). On the other hand, Huang et al. (2009) simply scratched the existing SiO_2/Si wafers by a diamond blade and passed ethanol over it at 900°C for 10 min. Bunch of SWCNTs grew on the scratched portions. Random scratches on thin SiO_2 films protrude some nanoparticles mechanically. These developments raise many new questions and compel us to reconsider the existing CNT-growth models. SiO_2 has no carbon solubility; how does it assist hydrocarbon-to-CNT conversion? Does it act as a solid-state catalyst like nanodiamond? Or does it melt at 900°C as usual metal nanoparticles do? If it is in molten state, Si and O atoms might have some mobility thus creating a vacancy or dislocation which would attract hydrocarbon and cause dehydrogenation. If it is in solid state, it would be strained enough (high curvature at small particle size) and could possibly interact with hydrocarbon. It is also likely that it is in a quasi-liquid (or semi solid) state; slight distortion in its overall shape would develop some polarity on Si and O atoms, which could possibly facilitate dehydrogenation; and its fluctuating shape could act as a template for tubular graphite formation. These speculations evoke serious discussion. SiO_2 has a number of distinct crystalline forms. Si–O bond length and Si–O–Si bond angle vary significantly in different crystal forms (e.g., 154–171 pm, 140°–180°). Ab-initio calculations indicate that CNT-cap nucleation is influenced by solid-surface curvatures (Reich et al., 2006). More theoretical considerations and experimental verifications are sought for proper understanding of CNT growth on SiO_2 nanoparticles. It will take due time to come up with a convincing model; nevertheless, there is no doubt that metal-free CNT synthesis is a major breakthrough in CNT research, and it has opened a new avenue in nanotechnology.

2.6 New CNT precursors

Apart from the popular hydrocarbons mentioned in the section 2.1, CNTs have also been synthesized from many other organic compounds, especially from polymers. Carbonization (prolonged pyrolysis in vacuum to convert organic compounds into solid carbon) of polyacrylonitrile (Parthsarathy et al., 1995) and poly-furfuryl-alcohol (Kyotani et al., 1996) within nanoporous alumina templates resulted in thick CNTs. Reported in 1995-96, this was a multi-step tedious process requiring chemically-controlled monomer initiators to achieve polymerization. The field has matured enough and nowadays super-aligned highly-uniform CNTs can be produced from readily available polymers without taking pains for chemical initiators or catalysts. Recently, several polymer precursors, loaded on commercially-

available alumina templates of well-defined pore size, were carbonized (400–600°C for 3h) to obtain MWCNTs of desired diameter (Han et al., 2009). N-doped MWCNTs obtained from carbonization of polypyrrole within alumina and zeolite membranes have shown better hydrogen-storage capacity than pristine MWCNTs obtained from polyphenyl acetylene in the same conditions (Sankaran et al., 2008). As for SWCNT, pyrolysis of tripropylamine within the nanochannels (0.73 nm) of aluminophosphate crystals (AFI) resulted in the narrowest nanotubes (0.4 nm) (Tang et al., 1998). Later, several carbon precursors were pyrolyzed within the AFI channels and tetrapropylammonium hydroxide was found to yield high densities of 4Å CNTs with better crystallinity (Zhai et al., 2006). It is suggested that the number of carbon atoms in the precursor molecule influences the SWCNT packing density in the template channels.

Among other organic compounds, amino-dichloro-s-triazine, pyrolyzed on cobalt-patterned silica substrates, resulted in highly pure CNTs (Terrones et al., 1997) Almost contemporary, organometallic compounds such as metallocene (ferrocene, cobaltocene, nickelocene) (Sen et al., 1997) and nickel phthalocyanine (Yudasaka et al., 1997) were used as the carbon-cum-catalyst precursor; however, as-grown CNTs were highly metal-encapsulated and the yield was very low. Later, pyrolysis of thiophene with metallocene led to the formation of Y-junction CNTs (Satishkumar et al., 2000). Recently, high-temperature pyrolysis (1300°C) of simple saccharides (from table sugar (sucrose) to lactose) resulted in straight as well as helical MWCNTs (Kucukayan et al., 2008).

In 2001, high yield of CNTs was obtained from camphor, a tree product (Kumar et al., 2001). Since then the authors remained involved with this environment-friendly source of CNTs and established the conditions for growing MWCNTs (Kumar et al., 2002; 2003a), SWCNTs (Kumar et al., 2003b) and vertically-aligned CNTs on quartz and silicon substrates (Kumar et al., 2003c; 2004) by using ferrocene catalyst. Later, using Fe-Co catalyst impregnated in zeolite support, mass production of CNTs was achieved by camphor CVD (Kumar et al., 2008). MWCNTs were grown at a temperature as low as 550°C, whereas SWCNTs could be grown at relatively high (900°C) temperature. Because of very low catalyst requirement with camphor, as-grown CNTs are least contaminated with metal, whereas oxygen atom present in camphor helps in oxidizing amorphous carbon in-situ (Kumar et al., 2007). These features of camphor stimulated more in-depth, basic and applied research worldwide.

Camphor-grown CNTs were used as the anode of secondary lithium battery (Sharon et al., 2002). Andrews et al. (2006) investigated the effect of camphor's molecular structure on the CNT growth and quality. Yamada et al. (2006) studied camphor CVD with different ways of catalyst feeding and addressed catalyst activation/deactivation process for the synthesis of highly-dense aligned CNT arrays. Parshotam (2008) studied the effect of carrier gases (nitrogen, argon, argon-hydrogen mixture) as well as catalyst-support materials (SiO_2, Al_2O_3 and MgO) on the quality of camphor-grown CNTs. Antunes et al. (2010) carried out thermal annealing and electrochemical purification of camphor-grown CNTs. Tang et al. (2010) synthesized tree-like multi-branched CNTs from camphor and reported the effects of temperature, argon flow rate and catalyst concentration on the structure of as-grown carbon nanotrees. Musso et al. (2007) got 2.3 mm thick CNT mats at a high deposition rate of 500 nm/sec. Later, the same group published fluid-dynamic analysis of the carrier-gas flow for camphor-CVD system (Musso et al., 2008) and hydrogen-storage analysis of camphor-grown CNTs (Bianco et al., 2010). Thus, camphor has emerged as a promising and the most-efficient CNT precursor amongst the new/unconventional ones. Moreover, it has opened up a new avenue of exploring other botanical products as a CNT precursor. Appreciable efforts

have been made by Sharon and his coworkers who investigated the pyrolysis of a range of plant-based materials for this purpose (Sharon et al., 2006). Recently, high yields of aligned and non-aligned CNTs have also been reported from other plant-derived cheap raw materials such as turpentine (Afre et al., 2005) and eucalyptus oils (P. Ghosh et al., 2009). Most recently, Zhao et al. (2011) used sesame seeds as a CNT catalyst precursor. Sesame seed consists of uniform microcells containing an Fe-complex. During CVD at 800°C, this Fe-complex releases uniformly-distributed Fe nanoparticles, which efficiently catalyze the CNT growth.

Apart from the well-defined chemical reagents described above, CNTs have also been successfully and systematically synthesized from domestic fuels such as kerosene (Pradhan et al., 2002), liquefied petroleum gas (Qian et al., 2002) and coal gas (Qiu et al., 2006). More interestingly, there are scientific reports of CNT production from green grasses. Grass contains dense vascular bundles mainly composed of cellulose, hemicellulose and lignin. Rapid heat treatment of grass (600°C) in controlled-oxygen ambience dehydrates and carbonizes the vascular bundles into CNTs (Kang et al., 2005). Thus, now it is almost certain that any carbon-containing material may be a CNT precursor under suitable experimental conditions. The point is: can we reproduce the product quality and quantity from those materials of inconsistent composition? Certainly not. Depending upon the chemical composition of the raw material, one will have to change the experimental conditions every now and then; and the impurity elements of the raw material would greatly contaminate the resulting CNTs which would ultimately be of no practical importance. Hence, seemingly novel and interesting research of CNT production from abundant materials, such as waste plastics or domestic garbage, would be a too-long-term project. To meet the immediate need of mass production of CNTs, it is advisable to choose a raw material of consistent chemistry, which is abundant and regenerative too; so that it could lead to a reproducible as well as sustainable industrial technique.

3. CNT growth mechanism

CNT growth mechanism has been debatable right from its discovery. Based on the reaction conditions and post-deposition product analyses, several groups have proposed several possibilities which are often contradicting. Therefore, no single CNT growth mechanism is well established till date. Nevertheless, widely-accepted most-general mechanism can be outlined as follows. A hydrocarbon vapor when comes in contact with the "hot" metal nanoparticles, first decomposes into carbon and hydrogen species; hydrogen flies away and carbon gets dissolved into the metal. After reaching the carbon-solubility limit in the metal at that temperature, as-dissolved carbon precipitates out and crystallizes in the form of a cylindrical network having no dangling bonds and hence energetically stable. Hydrocarbon decomposition (being an exothermic process) releases some heat to the metal's exposed zone, while carbon crystallization (being an endothermic process) absorbs some heat from the metal's precipitation zone. This precise thermal gradient inside the metal particle keeps the process on.

Now there are two general cases. (Fig. 3a) When the catalyst-substrate interaction is weak (metal has an acute contact angle with the substrate), hydrocarbon decomposes on the top surface of the metal, carbon diffuses down through the metal, and CNT precipitates out across the metal bottom, pushing the whole metal particle off the substrate (Fig. 3a(i)). As long as the metal's top is open for fresh hydrocarbon decomposition, the concentration gradient exists in

the metal allowing carbon diffusion, and CNT continues to grow longer and longer (Fig. 3a(ii)). Once the metal is fully covered with excess carbon, its catalytic activity ceases and the CNT growth is stopped (Fig. 3a(iii)). This is known as "tip-growth model".
In the other case, (Fig. 3b) when the catalyst-substrate interaction is strong (metal has an obtuse contact angle with the substrate), initial hydrocarbon decomposition and carbon diffusion take place similar to that in the tip-growth case, but the CNT precipitation fails to push the metal particle up; so the precipitation is compelled to emerge out from the metal's apex (farthest from the substrate, having minimum interaction with the substrate). At first, carbon crystallizes out as a hemispherical dome (the most favorable closed-carbon network on a spherical nanoparticle) which then extends up in the form of seamless graphitic cylinder. Subsequent hydrocarbon decomposition takes place on the lower peripheral surface of the metal, and as-dissolved carbon diffuses upward. Thus CNT grows up with the catalyst particle rooted on its base; hence, this is known as "base-growth model".
However, there are several points of discord in the above-mentioned *general* CNT growth mechanism. We are not sure that, during the CNT growth, whether the metal is in solid or liquid state, whether the carbon diffusion in metal is volume diffusion or surface diffusion, whether the actual catalyst for CNT growth is the pure metal or metal carbide, etc. Let us now review some important in-situ electron microscopic studies on these aspects.

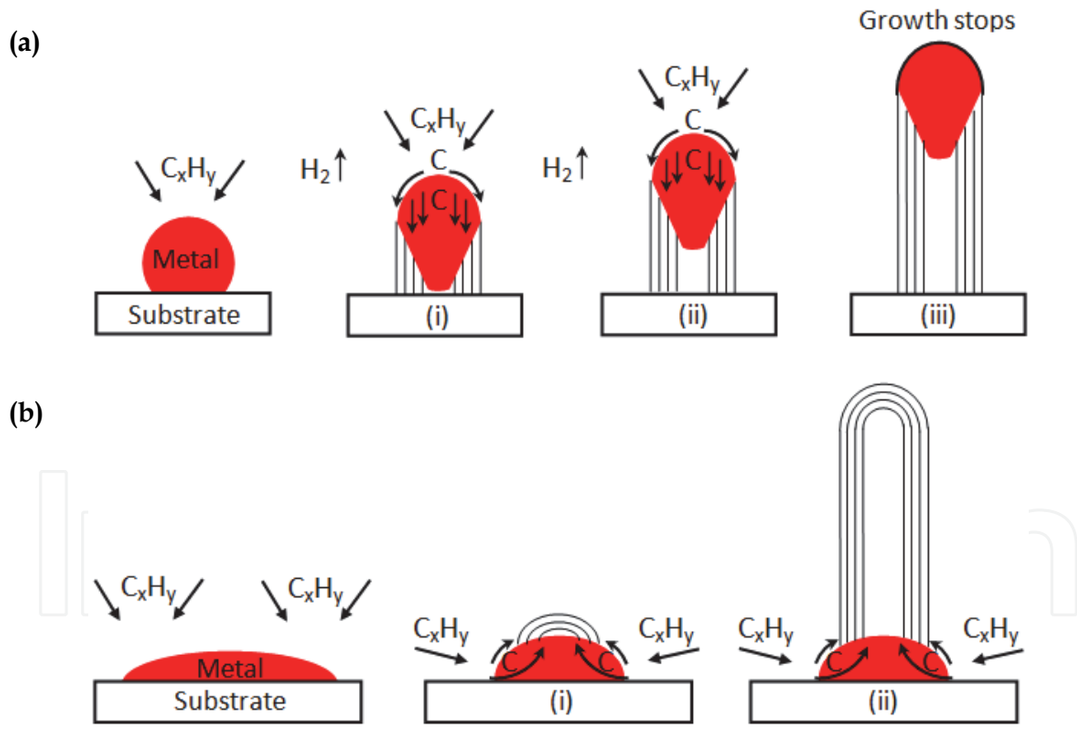

Fig. 3. Widely-accepted growth mechanisms for CNTs: (a) tip-growth model, (b) base-growth model.

3.1 Physical state of the catalyst

The first effort to observe the carbon filament growth process in-situ was made by Baker et al. (1972). By installing a gas-reaction cell in the TEM specimen chamber, they were able to

perform carbon fiber growth in a temperature range of 600–1200°C at different gas pressures up to 225 torr (maximum), while the TEM column was maintained at sufficiently low temperature and pressure suitable for electron microscopy. For acetylene decomposition on nickel catalyst supported on silica and graphite supports at 600°C, they clearly observed that the metal particles changed it shape and moved up with a trail of carbon deposit (30–50 nm diameter). From the changing shape of the metal particle during fiber growth, they assumed that the catalyst was in liquid phase. The activation energy calculated for this growth was nearly same as the activation energy of carbon diffusion in liquid nickel; hence they suggested that carbon diffuses through the bulk metal and the fiber growth rate is diffusion-controlled. Similar tip-growth process was observed with Fe, Co and Cr catalysts (Baker et al., 1973). But in the case of acetylene decomposition on bimetallic (Pt-Fe) catalyst, the catalyst was observed to remain static on the substrate, while the carbon filament went on growing up. This led them to enunciate a base-growth model (Baker et al., 1975). It was explained that strong interaction between Pt-Fe and SiO_2 substrate kept the metal particle anchored to the substrate surface, and carbon precipitation occurred from the free upper face of the particle. Temperature and concentration gradients were thought to be the main driving forces for the continued growth dynamics. The filament growth was seen to be ceased when the particle was fully covered with the carbon cloud, but it could be re-activated by exposure to either hydrogen or oxygen at higher temperatures (Baker et al., 1972). Later, however, many scientists reported base-grown CNTs from Fe and Co catalysts on Si and SiO_2 substrates (Li et al., 1999; Bower et al., 2000). This indicates that the same set of hydrocarbon, catalyst and substrate may act differently in slightly different experimental conditions (temperature, pressure, etc.).

In 1984, Tibbetts explained why catalytically-grown carbon nanofibers were tubular. Because the surface free energy of the (002) basal plane of graphite is exceptionally low, the free energy required for a filament growth is minimum when graphite is in the form of a seamless cylinder circumfering the metal. And the inner core is hollow because inner cylindrical planes of small diameter would be highly strained, energetically unfavorable to form. He also explained the CNT growth mechanism with a vapor-liquid-solid (VLS) model, originally formulated for Si, Ge whiskers and many other crystals (Wagner et al., 1965). Although this model is convincing and acceptable to a great extent, it is often doubted how Fe, Co, Ni etc. (normal melting point ~1500°C) could be in liquid state within 600–900°C, the growth temperature of typical CNTs in CVD. Here it is important to note that the melting point of nanoparticles below 10 nm falls abruptly (Fig. 4). For instance, an 8-nm Fe and Au particle (or 4-nm Ni particle) can melt at about 800°C. Typical CNT growth temperature range is 700–900°C, implying that in some cases (>800°C) the catalyst metal may be in liquid state, while in some cases (<800°C) it may be in solid state. Also, in any experiment, all particles are not strictly of the same size. So, it is still hard to say on the metal's state authoritatively. However, recalling that hydrocarbon decomposition on metal surface is an exothermic reaction, it is likely that the extra heat generated during hydrocarbon decomposition helps metal liquefaction to some extent. Hence the opinion of active catalyst being in liquid phase wins, as reported by many scientists for SWCNT growth (Ding et al., 2004; Harutyunyan et al., 2005). But then, what about the case of MWCNTs which usually grow on bigger (>20 nm) metal particles? Bigger particles must be in solid phase; and in turn, MWCNT would involve a different growth mechanism than that of SWCNT!!

Another reasonable disagreement between the SWCNT and MWCNT growth is on the existence of temperature gradient inside the metal catalyst. Baker's explanation of

temperature-gradient driven fiber growth might be applicable to MWCNTs which involve big catalyst particles. In the case of SWCNTs, however, it is very hard to imagine a significant temperature gradient within a particle of 1-2 nm. Hence SWCNT growth must be driven by the carbon concentration gradient during the process. A molecular dynamics simulation study suggests the possibility of SWCNT growth without any temperature gradient in the metal (Ding et al., 2006).

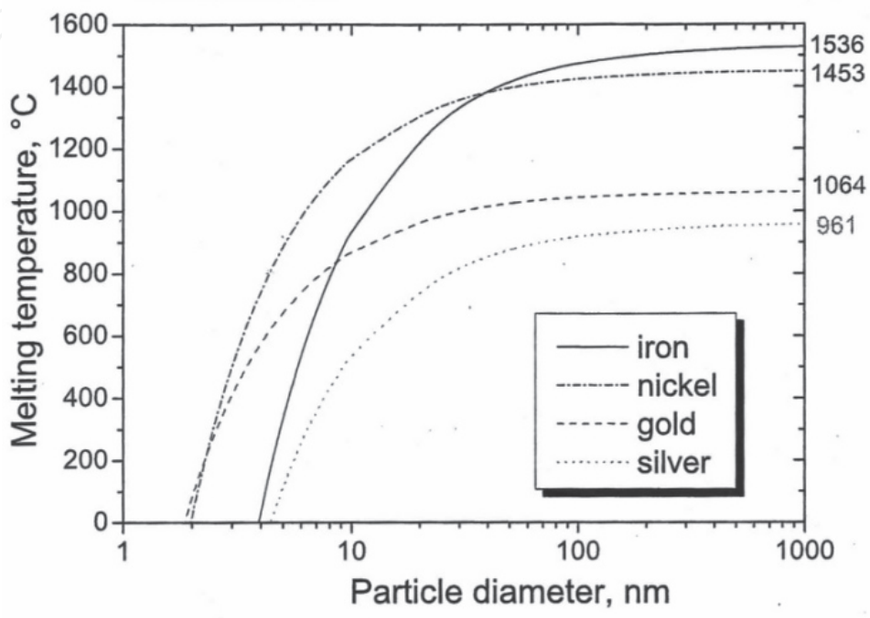

Fig. 4. Melting temperature of selected metals as a function of particle diameter. (Moisala et al., 2003. *J. Phys.: Condens. Mater.* 15, S3011-S3035. © IOP Publishing Ltd.)

3.2 Mode of carbon diffusion

Another highly-debatable question is whether the so-called diffusion of carbon species through metal particle is surface diffusion or bulk (volumetric) diffusion. Endo's group who extensively carried out benzene decomposition on iron catalyst at 1100°C (Oberlin et al., 1976), argued that hollow fiber could form only by surface diffusion on the metal particle, as earlier proposed by Baird et al. (1971). In 2004, Helveg et al. succeeded in observing MWCNT growth from methane decomposition at 500°C on Ni catalyst in a high-resolution TEM. They noted that, throughout the growth process, the nickel cluster remained crystalline with well-faceted shapes (Fig. 5). The graphite layers were found to grow as a consequence of dynamic interaction between carbon and nickel atoms. 'Surface atoms' of the nickel cluster moved up and down, in and out (continuously changing the metals' surface texture) as if they were knitting a graphene sheet out of the surrounding carbon atoms. The nanocluster shape was periodically changing its shape from spherical to cylindrical, aligning the graphene layers around them. The authors proposed that the mono-atomic steps on the cluster boundary played a key role in anchoring carbon atoms and knitting the graphene network. This observation reveals that the catalyst is in solid phase and the carbon diffusion is a surface diffusion around the catalyst.

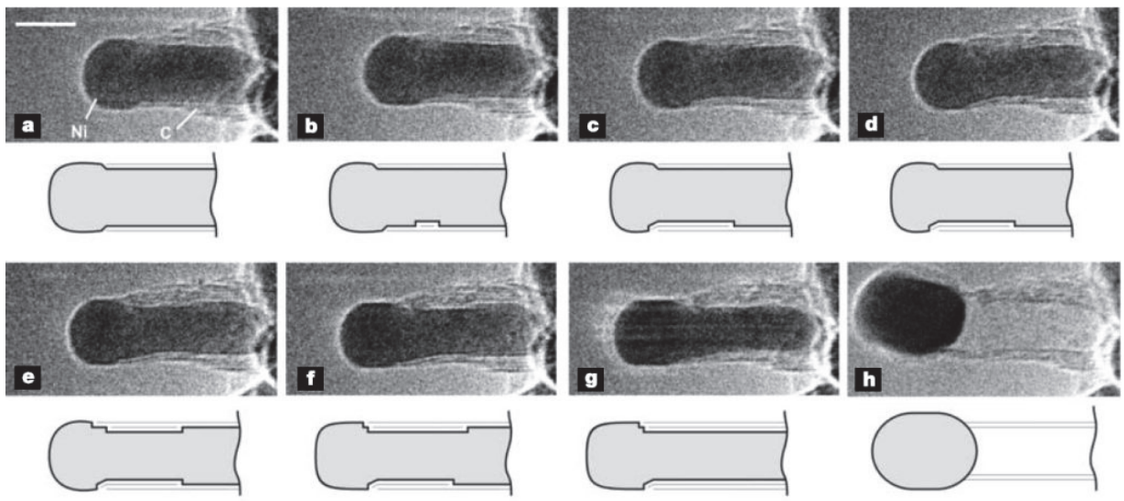

Fig. 5. In situ HRTEM image sequence of a growing carbon nanofiber. Images (a–h) illustrate one cycle in the elongation/contraction process. Drawings are included to guide the eye in locating the positions of mono-atomic Ni step-edges at the graphene–Ni interface. Scale bar = 5 nm. (Helveg et al., 2004. *Nature* 427, 426-429. © Nature Publishing Group)

Later, Raty et al. (2005) reported a molecular dynamics simulation study of the early stages of SWCNT growth on metal nanoparticles. They showed that carbon atoms diffuse only on the outer surface of the metal cluster. At first, a graphene cap is formed which floats over the metal, while the border atoms of the cap remain anchored to the metal. Subsequently, more C atoms join the border atoms pushing the cap up and thus constituting a cylindrical wall (Fig. 6).

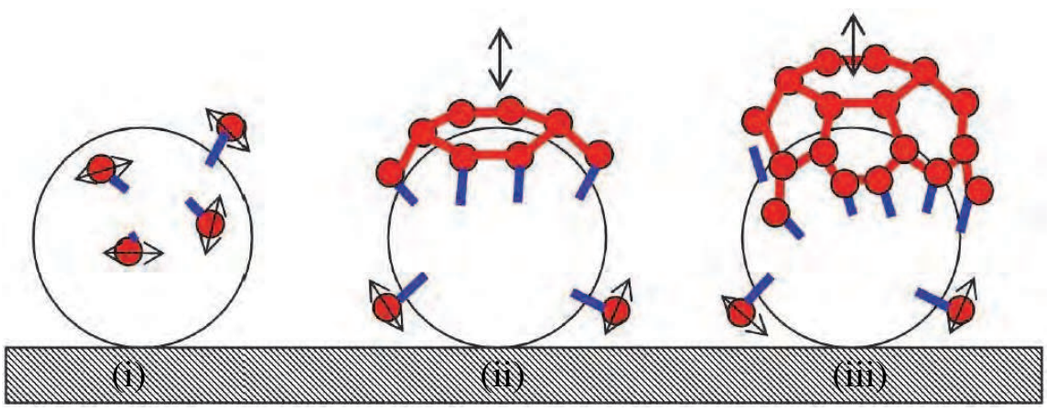

Fig. 6. Schematic representation of the basic steps of SWCNT growth on a Fe catalyst, as observed in *ab initio* simulations. (i) Diffusion of single C atoms (red spheres) on the surface of the catalyst. (ii) Formation of an sp^2 graphene sheet floating on the catalyst surface with edge atoms covalently bonded to the metal. (iii) Root incorporation of diffusing single C atoms. (Raty et al., 2005. *Phys. Rev. Lett.* 95, 096103. © American Physical Society)

In 2007, Hofmann et al. reported an atomic-scale environmental TEM observation of CNT growth from acetylene decomposition on Ni particles at 480°C. Figure 7 shows the growth stage at different times (as mentioned therein) captured from a continuous video recording.

Initially, the Ni cluster had a round shape which transformed into an elongated shape (perpendicular to the substrate) surrounded by a thin carbon layer. This elongation was in contact with the substrate up to 0.8s and suddenly (at 0.87s), the Ni cluster left the substrate contact and contracted upward taking a round shape and leaving behind a hollow carbon tube. This elongation and contraction of Ni re-occurred alternately, moving ahead and leaving behind a bamboo-like MWCNT grown. The inner walls of the tube appeared to emerge from step-like stages of Ni cluster (see HRTEM and corresponding model in Fig. 7), suggesting that carbon atoms also diffuse deep inside the Ni cluster and crystallize in the form of inner tube walls when the Ni cluster moves up (contracts back to round shape at the CNT tip). This was a MWCNT observation via tip growth model. In another experiment at 615°C, the authors observed SWCNT formation from a small Ni cluster via base growth model (Fig. 8). Initially, a carbon cap emerged with a diameter smaller than the Ni cluster. Then, the apex portion of the cluster assumed a cylindrical shape, pushing the carbon cap off the cluster and forming a SWCNT. Finally, the CNT network expanded upward by itself. These evidences also explain the general experience that small nanoparticles are crucial for SWCNT formation. Small metal clusters (1–2 nm) have sharp edges (atomic steps); hence they possess high catalytic activity and are capable to form high-strain SWCNTs. With the increasing cluster size, the sharpness of the atomic steps at the cluster boundary decreases and so does their catalytic activity. Therefore, bigger metal clusters (5–20 nm) form less-strained MWCNTs. Too big clusters (viz. 100 nm) acquire almost spherical boundary with no sharp steps; that is why they do not form CNTs at all.

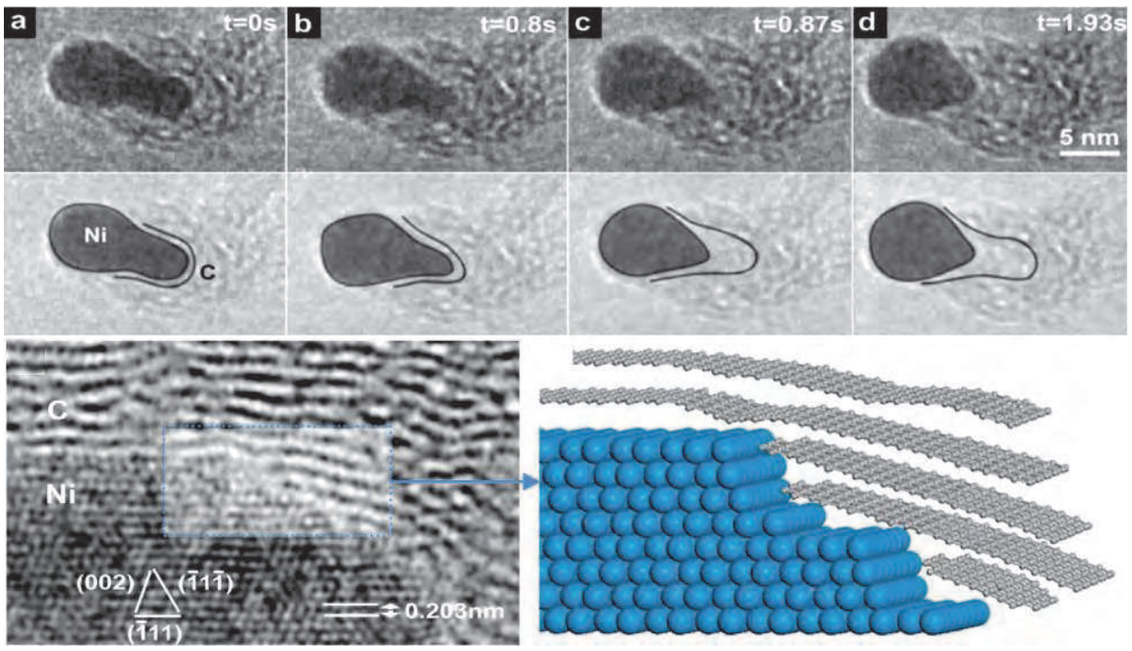

Fig. 7. In-situ TEM image sequence showing a MWCNT nucleation and growth, and corresponding growth scheme. (Hofmann et al., 2007. Nano Lett. 7, 602-608. © American Chemical Society)

Quite intriguingly, however, two months after Hofmann's (2007) report, Rodriguez-Manzo et al. (2007) reported an exciting observation of CNT formation in an HRTEM by simply holding a metal-encapsulated MWCNT at 600°C under electron beam (300kV) for 90 min. Carbon atoms from the side walls (the existing graphite layers around the encapsulated metal) got injected into the metal bulk and emerged in the form of new SW, DW and MWCNTs of smaller diameters coaxial to the original MWCNT (Fig. 9). Such a prolonged observation of the CNT-growth dynamics (atom-by-atom) clearly evidences that carbon diffuses through the metal bulk (volume diffusion). Nevertheless, we should note that this observation was an exclusive case of rearrangement of the carbon-iron ensemble inside a constrained nanoreactor (the original MWCNT) under high-energy electron-beam irradiation, a situation far away from usual CVD conditions. Hence such bulk diffusion cannot be conceptualized as a general CNT growth mechanism.

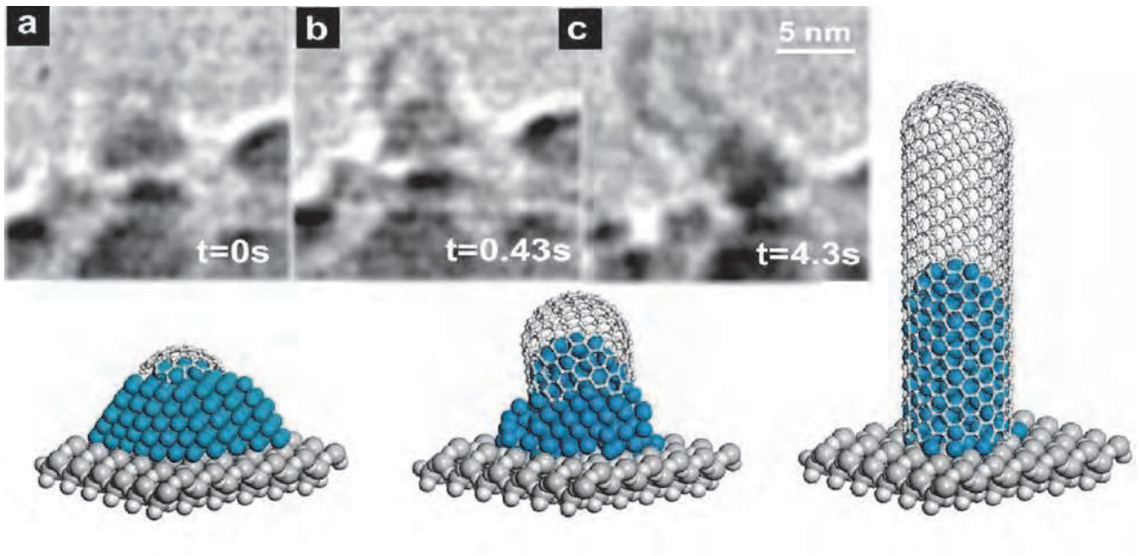

Fig. 8. In-situ TEM image sequence showing a SWCNT nucleation and growth, and corresponding growth scheme. (Hofmann et al., 2007. *Nano Lett.* 7, 602-608. © American Chemical Society)

In the context of the changing metal shape during CVD, it is pertinent to mention another aspect of the CNT growth. Many a time we encounter CNTs with their graphene layers inclined to the tube axis (herringbone or stacked-cup structure). It is puzzling to think how they form. Keeping in mind that graphite layers grow preferentially on selected crystal planes of metal, this can be understood as follows. The shape of the catalyst metal cluster acts as a template for the surrounding graphene layers. Nanoclusters (say, 10–20 nm Ø) under suitable thermodynamic conditions, tend to form an elongated cylindrical shape (viz., 3 nm Ø) so that CNTs grow with the graphene layers parallel to the tube axis. Under certain (different) thermodynamic conditions the metal clusters tend to become pear-shaped, giving birth to graphene layers parallel to their inclined facets. This usually happens with bigger clusters (say, 100 nm) or for alloy catalysts (Kim et al., 1992). When it comes to explain how such open-edged nanographenes are energetically stable, scientists suggest that those dangling bonds at the edges of the stacked graphite platelets are stabilized with the hydrogen atoms expelled from the hydrocarbon or from the H_2 supply (Nolan et al., 1998). Such a fiber is known as graphite whisker, and many people do not consider that as a CNT.

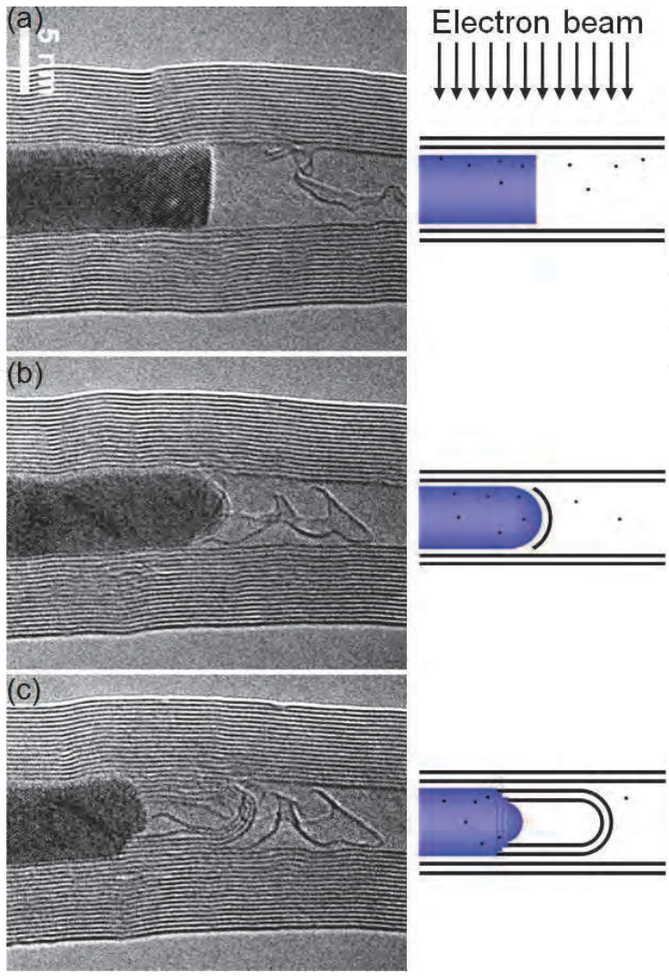

Fig. 9. In-situ observation of CNT growth under HRTEM. (a) Electron beam knocks some carbon atoms from the MWCNT side walls into the encapsulated metal cluster. (b) The metal cluster reshapes its flat cross section into a convex dome and a carbon cap appears over the dome. (c) At the base of the metal dome, atomic steps develop and new MWCNTs emerge coaxial to the original MWCNT. (Image courtesy: M. Terrones)

3.3 Chemical state of the catalyst

Another frequently debated point in the CNT growth mechanism is about the chemical state of the active catalyst. Most common concept is that the starting catalyst material (pre-deposited on substrates) is usually in oxide form. Even if we deposit fresh metal nanoparticles on a substrate, the nanoparticles get quickly oxidized when exposed to oxygen during the substrate transfer to the CVD reactor. During CVD, hydrogen gas is supplied to reduce the metal oxide into pure metal upon which hydrocarbon decomposition and subsequent diffusion leads to the CNT growth. Even when no hydrogen is supplied externally, the hydrogen atoms liberated from the hydrocarbon decomposition on the catalyst surface are likely to serve the same. However, there are many conflicting reports right from the early-stage CVD experiments. Baker and many others proposed that pure metal is the active catalyst (Baker et al., 1982; Yang et al., 1986), while Endo and many others

detected the encapsulated particles (in the CNTs) to be iron carbide (Oberlin et al., 1976; Ducati et al., 2004).

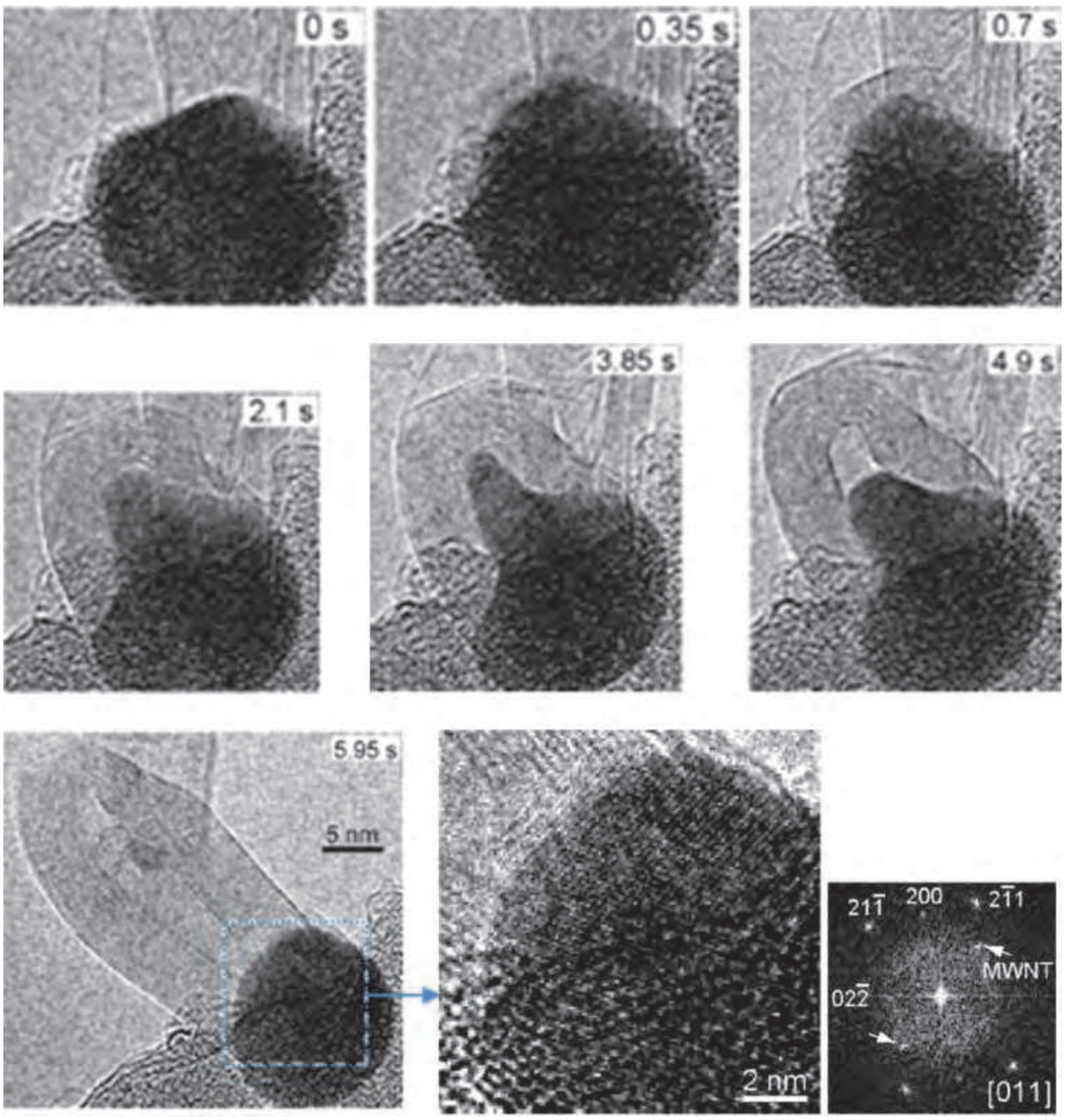

Fig. 10. In-situ TEM observation of MWCNT nucleation and growth as a consequence of acetylene decomposition on iron catalyst at 600°C. Initially, graphene layers appear around the metal cluster. Subsequently, the metal cluster assumes a conical shape, elongates upward (expelling a CNT), and finally, comes back to round shape. Fourier transform of the enlarged image of the metal cluster at 5.96s suggests it to be Fe_3C. (Yoshida et al., (2008). *Nano Lett.* 8, 2082-2086. © American Chemical Society)

In 2008, Yoshida et al. performed atomic-scale in-situ observation of acetylene decomposition on Fe catalyst at 600°C and 10^{-2} torr. Both SWCNT and MWCNT were clearly observed to be growing from metal particles rooted on the substrate (base-growth model). Electron diffraction analysis of the metal clusters in each frame was reported to match with that of iron carbide in cementite (Fe_3C) form (Fig. 10). Accordingly, the authors concluded that the active catalyst was in 'fluctuating solid state' of 'iron carbide'; the carbon diffusion was volumetric; and all layers of the MWCNTs grew up simultaneously, at the same growth rate.

However, Wirth et al. (2009), based on their in-situ electron microscopy and XPS analyses, emphatically advocate that the catalyst exists in pure metallic form: right from the CNT nucleation to the growth termination (Fig. 11). When the CNT growth ceases due to catalyst poisoning with excess carbon, that supersaturated metal-carbon assembly crystallizes in carbide form upon cooling. Confusion persists because lattice constants of pure metal and their carbide or oxide are very close. For instance, 2Å reflection is possible from fcc Ni(111) or Ni_3C(113) or Ni_2O_3(200). Moreover, for 'nano' particles, some distortion in the lattice constants is expected due to the small-size effect. The authors also suggest that the catalyst particle undergoes severe mechanical re-shaping during the tip growth of multi-wall nanotubes. This looks like the metal is in liquid state. However, this shape distortion occurs due to relative displacement of different atomic layers (in solid state) due to the large forces exerted by the surrounding CNT in the growth stage.

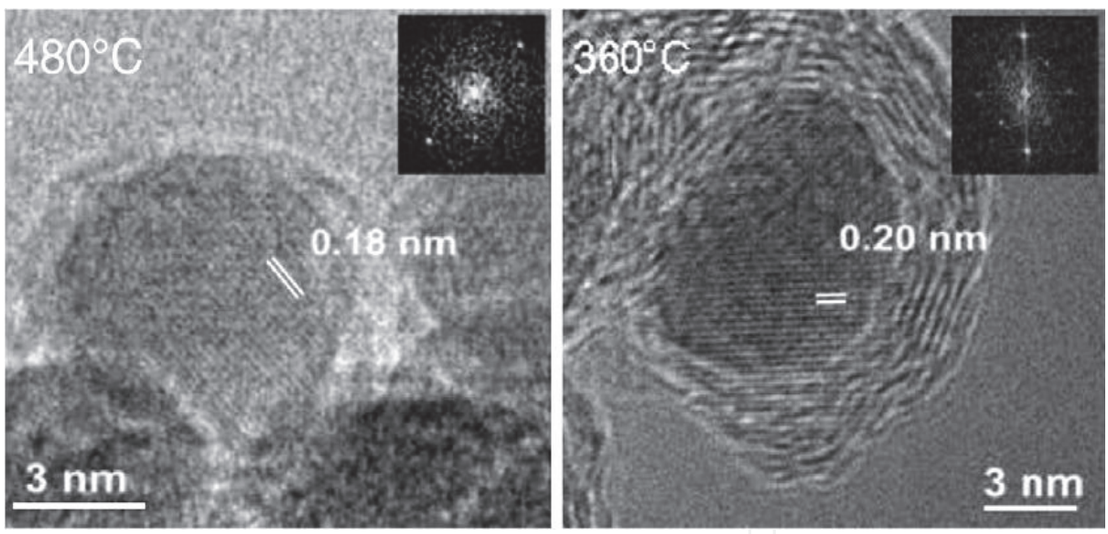

Fig. 11. In-situ TEM images of CNT growth from acetylene decomposition on Ni particles at 480 °C and 360°C. Clear observation of lattice planes suggests the metal to be in crystalline (solid) state. (Wirth et al., 2009. *Diamond & Related Mater.* 18, 940-945. © Elsevier Science)

Among the latest literature, Chen et al. (2011) performed in-situ resonance Raman spectroscopy and XRD photoelectron spectroscopy of ethanol CVD directly on SiO_2 nanoparticles without any metal. Their results suggest that, during the CVD, SiO_2 does not form any SiC phase and the SWCNT nucleation and growth occur by carbon diffusion on solid SiO_2 particles, following a vapor-solid-solid (VSS) model, instead of the conventional vapor-liquid-solid (VLS) model (Fig. 12).

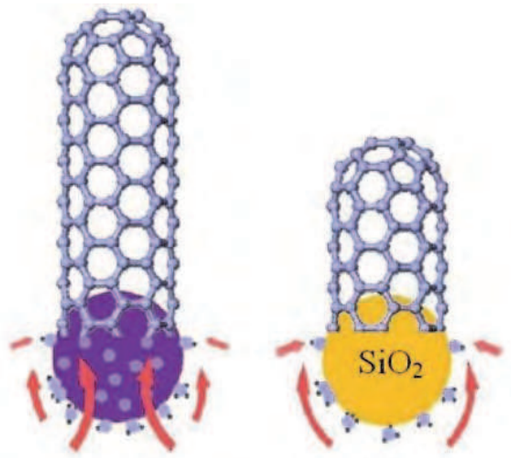

Fig. 12. (a) VLS model for SWCNT growth from a metal nanoparticle: volume diffusion of C atoms (vapor) in metal (liquid) to crystallize a CNT (solid). (b) VSS model for the SWCNT growth from an SiO_2 nanoparticle: surface diffusion of carbon atoms (vapor) on SiO_2 (solid) resulting in a CNT (solid). (Chen et al., 2011. *Carbon* 49, 3316-3324. © Elsevier Science)

These diversities of observation unambiguously reflect that we have not matured enough to understand the world inside the nanotubes. Hence more research is required to establish a concrete growth mechanism. Then only we would be able to make CNTs of specific properties, and in turn, CNT would be able to fulfill the expectations and needs of the society.

4. Existing challenges and future directions

In the foregoing sections, we raised several questions on the roles of precursor, catalyst, catalyst support and growth mechanism, and indicated possible directions. In addition to those basic issues, other growth-related challenges are briefly outlined below.

1. Researchers have succeeded in minimizing the diameter distribution of SWCNTs up to some extent. However, synthesis of SWCNTs of a given diameter is yet to be achieved. It would be possible only when we have the catalyst particles all of exactly the same diameter (say, 0.5 nm).
2. Chirality control is even more challenging. Re-growth from ordered arrays of open-ended SWCNTs may help up to some extent. Alternatively, we have to develop proper separation methods that could first sort out CNTs according to metallic or semiconducting tubes and then select tubes of specific chirality.
3. In MWCNTs, control on the number of walls is another big challenge. Synthesis of thin MWCNTs (3–6 walls) is a better choice than thick MWCNTs.
4. Growth of isolated CNTs has not yet reached a mature stage. There are indications that even a single CNT does not possess the same diameter and chirality over the entire length. How can we solve it?
5. Researchers have succeeded in growing CNTs from almost all metals. However, we do not know how different metals affect the physical, chemical, electronic and optical and magnetic properties of as-grown CNTs. If we could discover any correlation between

the type of the metal used and the property of the CNT grown, we would be able to grow CNTs of selective properties.

6. What is/are the determining steps in CNT nucleation and growth? Having known these steps, the CNT growth rate could be increased for mass production.
7. The exact role of H_2, O_2 and H_2O in CNT growth is yet to be clarified. Simultaneous presence of reducing as well as oxidizing agents in the reaction zone makes it ambiguous whether amorphous carbon is etched by atomic hydrogen, oxygen or water. Are they really essential?
8. Researchers have succeeded in bringing down the CNT growth temperature to ~400°C in low-pressure CVD. However, low-pressure CVD greatly reduces the growth rate and yield. Low-temperature CNT growth must be devised at atmospheric pressure for high yields of CNTs.
9. Many technological applications are looking for room-temperature CNT growth which is still a dream, so far as thermal CVD is concerned.
10. Mass-produced CNTs usually contain catalyst particles or support materials as impurity. Post-deposition purification greatly reduces the CNT quality and final output.
11. CVD-grown CNTs (especially low-temperature MWCNTs) have poor crystallinity. With a suitable combination of different catalysts, it should be possible to get better-crystallinity CNTs.
12. Recent metal-free oxygen-assisted CNT growth is a breakthrough. It must be scaled up to mass production of high-purity CNTs.
13. Carbon-metal phase diagram needs to be reconstructed, especially for 1–5 nm range, relevant to CNT growth.
14. All extraordinary properties of CNTs are predicted for atomically-perfect CNTs. To make those predictions true, it is of prime importance to develop new techniques to monitor and remove defects during the growth.
15. Lack of the quality control and assessment of the CNTs synthesized by different groups by different methods does not allow us to get the correct product details. Analytical sampling of CNTs obtained from different sources at an authorized standard laboratory would reveal exact merits and demerits of different techniques, which would in turn help us explore combinations of techniques toward high-yield, high-purity and low-cost mass production.

5. Conclusion

As we have seen in the foregoing sections, despite extensive progress over the years, there are many basic issues concerning the CNT growth mechanism which are still not clear. Contradictory observations of CNT growth under electron microscopy by different groups suggest that the mechanism is extremely sensitive to each parameter such as carbon precursor, metal catalyst, particle size, temperature, pressure. Even a minor change in any of these parameters leads the growth in critically different directions. Catalysis is the main stem of CVD-CNT technique; and it seems that we have not yet utilised the best of catalysis in this field. New nano-catalyst materials are needed to be developed and investigated in more detail. In principle, with the use of a suitable catalyst, the CVD temperature can be brought down to room temperature. By identifying the growth-limiting steps it should be possible to control the diameter and chirality of the resulting CNTs. To comply with the

environmental concerns, renewable materials should be explored as CNT precursors. In view of the expected giant demand of CNTs in the near future, industrial production of CNTs should be carried out with far-sighted thoughts for long-term sustainability. Fossil-fuel based CNT-production technology would not be sustainable. The unanswered questions about growth mechanism and the existing problems concerning the growth control will keep the CNT researchers engaged for a long time. Thus, there is no doubt that CNT research will continue to remain a hot topic, a prospective research area.

6. References

Afre R.A., Soga T., Jimbo T., Kumar M., Ando Y. and Sharon M. (2005). *Chem. Phys. Lett.* 414, 6-10.

Andrews R.J., Smith C.F. and Alexander A.J. (2006). *Carbon* 44, 341-347.

Antunes E.F., Almeida E.C., Rosa C.B.F., Medeiros L.I., Pardini L.C., Massi M. and Corat E.J. (2010). *J. Nanosci. Nanotechnol.* 10, 1296-1303.

Baird T., Fryer J.R. and Grant B. (1971). *Nature* 233, 329-330.

Baker R.T.K., Barber M.A., Harris P.S., Feates F.S. and Waite R.J. (1972). *J. Catalysis* 26, 51-62.

Baker R.T.K., Harris P.S., Thomas R.B. and Waite R.J. (1973). *J. Catalysis* 30, 86-95.

Baker R.T.K. and Waite R. J. (1975). *J. Catalysis* 37, 101-105.

Baker R.T.K., Alonzo J.R., Dumesic J.A. and Yates D.J.C. (1982). *J. Catalysis* 77, 74-84.

Bianco S., Giorcelli M., Musso S., Castellino M., Agresti F., Khandelwal A., Russo S.L., Kumar M., Ando Y. and Tagliaferro A. (2010). *J. Nanosci. Nanotechnol.* 10, 3860-3866.

Bower C., Zhou O., Zhu W., Werder D.J. and Jin S. (2000). *Appl. Phys. Lett.* 77, 2767-2769.

Camilli L., Scarselli M., Gobbo S.D., Castrucci P., Nanni F., Gautron E., Lefrant S. and Crescenzi M.D. (2011). *Carbon* 49, 3307-3315.

Cassell A.M., Raymakers J.A., Kong J. and Dai H., (1999). *J. Phys. Chem. B* 103, 6484-6492.

Chen Y. and Zhang J. (2011). *Carbon* 49, 3316-3324.

Dai H., Rinzler A.G., Nikolaev P., Thess A., Colbert D.T. and Smalley R.E. (1996). *Chem. Phys. Lett.* 260, 471-475.

Ding F., Bolton K. and Rosen A. (2004). *J. Chem. Phys. B* 108, 17369-17377.

Ding F., Bolton K. and Rosen A. (2006). *Comput. Mater. Sci.* 35, 243-246.

Ding F., Larsson P., Larsson J.A., Ahuja R., Duan H., Rosen A. and Bolton K. (2008). *Nano Lett.* 8, 463-468.

Ducati C., Alexandrou I., Chhowalla M., Robertson J. and Amaratunga G.A.J. (2004). *J. Appl. Phys.* 95, 6387-6391.

Endo M., Fujiwara H. and Fukunaga E. (1991). 18th Meeting Japanese Carbon Society Saitama (Dec 1991) p34.

Fan S., Chapline M., Frankline N., Tombler T., Cassell A.M. and Dai H. (1999). *Science* 283, 512-514.

Ghosh K., Kumar M., Maruyama T. and Ando Y. (2009). *Carbon* 47, 1565-1575.

Ghosh P., Soga T., Tanemura M., Zamri M., Jimbo T., Katoh R. and Sumiyama K. (2009). *Appl. Phys. A* 94, 51-56.

Han C.Y., Xiao Z.L., Wang H.H., Lin X.M., Trasobares S. and Cook R.E. (2009). *J. Nanomaterials* 2009, 562376(11pages).

Han S., Liu X. and Zhou C. (2005). *J. Am. Chem. Soc.* 127, 5294-5295.

Harutyunyan A.R. and Tokune T. (2005). *Appl. Phys. Lett.* 87, 51919-15921.

Hata K., Futaba D.N., Mizuno K., Namai T., Yumura M. and Iijima S. (2004). *Science* 306, 1362-1364.

He D., Li H., Li W., Haghi-Ashtiani P., Lejay P. and Bai J. (2011). *Carbon* 49, 2273-2286.

Helveg S., Lopez-Cartes C., Sehested J., Hansen P.L., Clausen B.S., Rostrup-Nielsen J.R., Abild-Pedersen F. and Nørskov J.K. (2004). *Nature* 427, 426-429.

Hofmann S., Sharma R., Ducati C., Du G., Mattevi C., Cepek C., Cantoro M., Pisana S., Parvez A., Cervantes-Sodi F., Ferrari A.C., Dunin-Borkowski R., Lizzit S., Petaccia L., Goldoni A. and Robertson J. (2007) *Nano Lett.* 7, 602-608.

Huang S., Cai Q., Chen J., Qian Y. and Zhang L. (2009). *J. Am. Chem. Soc.* 131, 2094-2095.

Iijima S. (1991). *Nature* 354, 56-58.

Jose-Yacaman M., Miki-Yoshida M., Rendon L. and Santiesteban J. G., (1993). *Appl. Phys. Lett.* 62, 657-659.

Kang Z., Wang E., Mao B., Su Z., Chen L. and Xu L. (2005). *Nanotechnology* 16, 1192-1195.

Kim M.S., Rodriguez N.M. and Baker R.T.K. (1992) *J. Catalysis* 134, 253-268.

Kucukayan G., Kayacan S., Baykal B. and Bengu E. (2008). *Mater. Res. Soc. Symp. Proc. (Symposium-P)* Vol. 1081E, P05-14.

Kumar M., Zhao X. and Ando Y. (2001). *International Symposium on Nanocarbons, Nagano, Japan (November 14-16, 2001) Extended Abstract*: 244-245.

Kumar M., Zhao X., Ando Y., Iijima S., Sharon M. and Hirahara K. (2002). *Mol. Cryst. Liq. Cryst.* 387, 117-121.

Kumar M. and Ando Y. (2003a). *Diamond Related Mater.* 12, 998-1002.

Kumar M. and Ando Y. (2003b). *Diamond Related Mater.* 12, 1845-1850.

Kumar M. and Ando Y. (2003c). *Chem. Phys. Lett.* 374, 521-526.

Kumar M., Kakamu K. Okazaki T. and Ando Y. (2004). *Chem. Phys. Lett.* 385, 161-165.

Kumar M. and Ando Y. (2005). *Carbon* 43, 533-540.

Kumar M., Okazaki T. Hiramatsu M. and Ando Y. (2007). *Carbon* 45, 1899-1904.

Kumar M. and Ando Y., (2008). *Defence Science Journal* 58, 496-503.

Kusunoki M., Suzuki T., Hirayama T. and Shibata N. (2000). *Appl. Phys. Lett.* 77, 531-533.

Kyotani T., Tsai L.F. and Tomita A. (1996). *Chem. Mater.* 8, 2109-2113.

Li J., Papadopoulos C., Xu J.M. and Moskovits M. (1999). *Appl. Phys. Lett.* 75, 367-369.

Li N., Chen X., Stoica L., Xia W., Qian J., Abmann J., Schuhmann W. and Muhler M. (2007). *Adv. Mater.* 19, 2957-2960.

Liu B., Ren W., Gao L., Li S., Pei S., Liu C., Jiang C. and Cheng H.M. (2009). *J. Am. Chem. Soc.* 131, 2082-2083.

Liu H., Takagi D., Chiashi S. and Homma Y. (2010). *Carbon* 48, 114-122.

Maret M., Hostache K., Schouler M.C., Marcus B., Roussel-Dherbey F., Albrecht M. (2007). *Carbon* 45, 180–187.

Maruyama S., Kojima R., Miyauchi Y., Chiashi S. and Kohno M. (2002). *Chem. Phys. Lett.* 360, 229-234.

Mattevi C., Wirth C.T., Hofmann S., Blume R., Cantoro M., Ducati C., Cepek C., Knop-Gericke A., Milne S., Castellarin-Cudia C., Dolafi S., Goldoni A., Schloegl R. and Robertson J. (2008). *J. Phys. Chem. C* 112, 12207-12213.

Merchan-Merchan W., Savaliev A., Kennedy L.A. and Fridman A. (2002). *Chem. Phys. Lett.* 354, 20-24.

Moisala A., Nasibulin A.G. and Kauppinen E.I. (2003). *J. Phys. Condens. Mater.* 15, S3011-S3035.

Murakami Y., Chiashi S., Miyauchi Y., Hu M., Ogura M., Okubo T. and Maruyama S. (2004). *Chem. Phys. Lett.* 385, 298-303.
Musso S., Porro S., Giorcelli M., Chiodoni A., Ricciardi A.C. and Tagliaferro A. (2007). *Carbon* 45, 1133-1136.
Musso S., Porro S., Rovere M., Giorcelli M. and Tagliaferro A. (2008). *J. Cryst. Growth* 310, 477-483.
Nerushev O.A., Dittmar S., Morjan R.E., Rohmund F. and Campbell E.E.B. (2003). *J. Appl. Phys.* 93, 4185-4190.
Noda S., Hasegawa K., Sugime H., Kakehi K., Zhang Z., Maruyama S. and Yamaguchi Y. (2007). *Jpn. J. Appl. Phys.* 46, L399-L401.
Nolan P.E., Lynch D.C. and Cutler A.H. (1998). *J. Phys. Chem. B* 102, 4165-4175.
Nunez J.D., Maser W.K, Mayoral M.C., Andres J.M. and Benito A.M. (2011). *Carbon* 49, 2483-2491.
Oberlin A., Endo M. and Koyama T. (1976). *J. Cryst. Growth* 32, 335-349.
Parshotam H. (2008). *M.Tech. Thesis, Chem. Dept., University of Johannesburg*.
Parthasarathy R.V., Phani K.L.N. and Martin C.R. (1995). *Adv. Mater.* 7, 896-897.
Pradhan D. and Sharon M. (2002). *Mater. Sci. Engg. B* 96, 24-28.
Qian W., Yu H., Wei F., Zhang Q. and Wang Z. (2002). *Carbon* 40, 2968-2970.
Qiu J., Li Q., Wang Z., Sun Y. and Zhang H. (2006). *Carbon* 44, 2565-2568.
Raty J.Y., Gygi F. and Galli G. (2005). *Phys. Rev. Lett.* 95, 096103(4pages).
Reich S., Li L. and Robertson J. (2006). *Chem. Phys. Lett.* 421, 469-472.
Ritschel M., Leonhardt A., Elefant D., Oswald S. and Buchner B. (2007). *J. Phy. Chem. C* 111, 8414-8417.
Rodriguez-Manzo J.A., Terrones M., Terrones H., Kroto H.W., Sun L. and Banhart F. (2007). *Nature Nanotechnology* 2, 307-311.
Rummeli M.H., Borowiak-Palen E., Gemming T., Pichler T., Knupfer M., Kalbac M., Dunsch L., Jost O., Silva S.R.P., Pompe W. and Buchner B. (2005). *Nano Lett.* 5, 1209-1215.
Rummeli M.H., Kramberger C., Gruneis A., Ayala P., Gemming T., Buchner B. and Pichler T. (2007a). *Chem. Mater.* 19, 4105-4107.
Rummeli M.H., Schaffel F., Kramberger C., Gemming T., Bachmatiuk A., Kalenczuk R.J., Rellinghaus B., Buchner B. and Pichler T. (2007b). *J. Am. Chem. Soc.* 129, 15772-15773.
Sankaran M. and Viswanathan B. (2008). *Indian J. Chem.* 47A, 808-814.
Satishkumar B.C., Thomas P.J., Govindaraj A. and Rao C.N.R. (2000). *Appl. Phys. Lett.* 77, 2530-2532.
Schneider J.J., Maksimova N.I., Engstler J., Joshi R., Schierholz R. and Feile R. (2008). *Inorganica Chimica Acta* 361, 1770-1778.
Sen R., Govindaraj A. and Rao C.N.R. (1997). *Chem. Phys. Lett.* 267, 276-280.
Sharon M., Hsu W.K., Kroto H.W., Walton D.R.M., Kawahara A., Ishihara T. and Takita Y. (2002). *J. Power Sources* 104, 148-153.
Sharon M. and Sharon M. (2006). *Synthesis and Reactivity in Inorganic, Metal-Organic and Nano-Metal Chemistry* 36, 265-279.
Su M., Li Y., Maynor B., Buldum A., Lu J.P., Liu J. (2000). *J Phys Chem B* 104, 6505–6508.
Takagi D., Hibino H., Suzuki S., Kobayashi Y. and Homma Y. (2007). *Nano Lett.* 7, 2272-2275.
Takagi D., Kobayashi Y., Hibino H., Suzuki S. and Homma Y. (2008). *Nano Lett.* 8, 832-835.
Takagi D., Kobayashi Y. and Homma Y. (2009). *J. Am. Chem. Soc.* 131, 6922-6923.

Tang J., Jin G., Wang Y. and Guo X. (2010). *Carbon* 48, 1545-1551.
Tang Z.K., Sun H.D., Wang J., Chen J. and Li G. (1998). *Appl. Phys. Lett.* 73, 2287-2289.
Terrones M., Grobert N., Olivares J., Zhang J.P., Terrones H., Kordatos K., Hsu W.K., Hare J.P., Townsend P.D., Prassides K., Cheetham A.K., Kroto H.W. and Walton D.R.M. (1997). *Nature* 388, 52-55.
Thess A., Lee R., Nikolaev P., Dai H., Petit P., Robert J., Xu C. and Smalley R. (1996). *Science* 273, 483-487.
Tibbetts G.G. (1984). *J. Cryst. Growth* 66, 632-638.
Vanderwal R.L., Ticich T.M. and Curtis V.E. (2001). *Carbon* 39, 2277-2289.
Wagner R.S. and Ellis W.C. (1965). *Trans. Metallurg. Soc. AIME* 233, 1053-1064.
Wirth C.T., Hofmann S. and Robertson J. (2009). *Diamond Related Mater.* 18, 940-945.
Xiang R., Einarsson E., Okawa J., Miyauchi Y. and Maruyama S., (2009). *J. Phys. Chem. C*, 113, 7511-7515.
Yamada K., Abe K., Mikami M., Saito M. and Kuwano J. (2006). *Key Engg. Mater.* 320, 163-166.
Yang K.L. and Yang R.T. (1986). *Carbon* 24, 687-693.
Yoshida H., Takeda S., Uchiyama T., Kohno H. and Homma Y. (2008). *Nano Lett.* 8, 2082-2086.
Yuan D., Ding L., Chu H., Feng Y., McNicholas T.P. and Liu J. *Nano Lett.* (2008). 8, 2576-2579.
Yudasaka M., Kikuchi R., Ohki Y. and Yoshimura S. (1997). *Carbon* 35, 195-201.
Zhai J., Tang Z., Sheng P. and Hu X. (2006). *IEEE Conf. 2006: (ICONN-2006)* 155-158.
Zhao J., Guo X., Guo Q., Gu L., Guo Y. and Feng F. (2011). *Carbon* 49, 2155-2158.
Zhong G., Hofmann S., Yan F., Telg H., Warner J.H., Eder D., Thomsen C., Milne W.I. and Robertson J. (2009). *J. Phys. Chem. C* 113, 17321-17325.
Zhou W., Han Z., Wang J., Zhang Y., Jin Z., Sun X., Zhang Y., Yan C. and Li Y. (2006). *Nano Lett.* 6, 2987-2990.

Carbon Nanotubes - Synthesis, Characterization, Applications

Edited by Dr. Siva Yellampalli

ISBN 978-953-307-497-9
Hard cover, 514 pages
Publisher InTech
Published online 20, July, 2011
Published in print edition July, 2011

Carbon nanotubes are one of the most intriguing new materials with extraordinary properties being discovered in the last decade. The unique structure of carbon nanotubes provides nanotubes with extraordinary mechanical and electrical properties. The outstanding properties that these materials possess have opened new interesting researches areas in nanoscience and nanotechnology. Although nanotubes are very promising in a wide variety of fields, application of individual nanotubes for large scale production has been limited. The main roadblocks, which hinder its use, are limited understanding of its synthesis and electrical properties which lead to difficulty in structure control, existence of impurities, and poor processability. This book makes an attempt to provide indepth study and analysis of various synthesis methods, processing techniques and characterization of carbon nanotubes that will lead to the increased applications of carbon nanotubes.

INTECH
open science | open minds

InTech Europe
University Campus STeP Ri
Slavka Krautzeka 83/A
51000 Rijeka, Croatia
Phone: +385 (51) 770 447
Fax: +385 (51) 686 166
www.intechopen.com

InTech China
Unit 405, Office Block, Hotel Equatorial Shanghai
No.65, Yan An Road (West), Shanghai, 200040, China
中国上海市延安西路65号上海国际贵都大饭店办公楼405单元
Phone: +86-21-62489820
Fax: +86-21-62489821

IntechOpen